Multi-omic and functional screening reveal targetable vulnerabilities in *TP53* mutated multiple myeloma

Short title: Novel vulnerabilities in *TP53* mutated myeloma

Dimitrios Tsallos[1], Nemo Ikonen[1], Juho J. Miettinen[1], Muntasir Mamun Majumder[1], Samuli Eldfors[1,2], Imre Västrik[1], Alun Parsons[1], Minna Suvela[1], Katie Dunphy[3], Paul Dowling[3], Despina Bazou[4], Peter O'Gorman[5], Juha Lievonen[6], Raija Silvennoinen[6], Pekka Anttila[6], Caroline A. Heckman[1]

1. Institute for Molecular Medicine Finland, Helsinki Institute of Life Science, University of Helsinki, iCAN Digital Precision Cancer Medicine Flagship, University of Helsinki, Helsinki, Finland;

2. Massachusetts General Hospital Cancer Center, Charlestown, MA, and Department of Medicine, Harvard Medical School, Boston, MA, USA;

3. *Department of Biology, Maynooth University, W23 F2K8, Maynooth, Ireland;*

4. School of Medicine, University College Dublin, D04 V1W8 Dublin, Ireland;

5. *Department of Haematology, Mater Misericordiae University Hospital, D07 WKW8, Dublin, Ireland;*

6. *Department of Hematology, Helsinki University Hospital Comprehensive Cancer Center, University of Helsinki, Helsinki, Finland*

Corresponding author:

Caroline A. Heckman, PhD

Institute for Molecular Medicine Finland – FIMM

University of Helsinki

Tukholmankatu 8 (P.O. Box 20)

FI-00290 Helsinki

Finland

c: +358 50 4156769

caroline.heckman@helsinki.fi

Abstract: 235 words

Text: 4324 words

Figures: 7 (5 figures and 2 tables)

References: 40

KEY POINTS

TP53 mutation in myeloma confers sensitivity to multiple compounds, including approved drugs, irrespective of del(17p) status.

TP53 mutated myeloma links to higher expression of drug targets involved in cell proliferation, mRNA processing, and chromatin modulation.

ABSTRACT

Despite development of several effective therapies for multiple myeloma (MM), the prognosis of patients with partial deletion of chromosome 17 (del(17p)) and *TP53* aberrations remains poor. By applying comprehensive multi-omics profiling analyses (whole exome and transcriptome sequencing plus proteomics) and functional *ex vivo* drug screening to samples from 167 patients with MM, we uncovered novel therapeutic vulnerabilities specific to *TP53* mutated MM. Our findings revealed a distinct sensitivity profile to a range of inhibitors (mitotic, topoisomerase, HDAC, HSP90, IGF1R and PI3K/AKT/mTOR inhibitors) irrespective of 17p deletion status. Conversely, no increase in sensitivity was observed for monoallelic *TP53* (del(17p) with WT *TP53*) when compared to WT *TP53* samples, highlighting the remaining unmet clinical need. Notably, plicamycin, an RNA synthesis inhibitor linked to modulation of chromatin structure and increased transcription, emerged as particularly efficacious for *TP53* mutated MM. The increased sensitivity correlated with higher protein expression of the drug targets: HDAC2, HSP90AA1 and multiple ribosomal subunits. Additionally, we observed increased RNA expression of G2M checkpoint, E2F targets and mTORC1 signaling in our cohort and the MMRF-CoMMpass (NCT01454297) study in *TP53* mutated MM. Harmonization of multi-omics data with *ex vivo* drug screening results revealed that *TP53* mutated MM is functionally distinct from MM with monoallelic *TP53*, and demonstrates that MM with mutated *TP53*, with and without del(17p), may be targetable by approved drugs. These results further indicate the need for regular monitoring by sequencing to identify these patients.

INTRODUCTION

Multiple myeloma (MM) is a complex and incurable disease characterized by a clonal proliferation of plasma cells in the bone marrow (BM). Significant advancements in MM treatment modalities have been made over the past decades[1], but despite the availability of novel treatments, the clinical and genetic heterogeneity of the disease continues to complicate prognosis and therapeutic strategies[1]. Genetic aberrations traditionally detected by fluorescence *in situ* hybridization (FISH) are known to play a pivotal role in MM progression and treatment outcomes[2]. Transitioning from FISH to next generation sequencing (NGS) could enhance the detection of recurrent aberrations to driver genes such as *TP53*, offering a more comprehensive genomic landscape and potentially refining therapeutic approaches and management of patients with MM[2].

Among the genetic aberrations influencing MM prognosis, deletion of the p arm of chromosome 17, del(17p), stands out as a high-risk factor with profound implications for patient prognosis and response to treatment[2,3]. Del(17p) is identified in 10% of patients with newly diagnosed MM and is primarily monoallelic. Importantly, the *TP53* gene is located within the minimally deleted region on 17p13. The co-occurrence of del(17p) together with *TP53* mutation, often referred to as 'double hit' MM, is associated with worse prognosis[2,3]. *TP53* mutations alone are detected in 1-7% of newly diagnosed patients with MM[4–6]. However, both *TP53* mutation and del(17p) aberrations are more prevalent after relapse occurring in approximately 23-45% of cases[5,7]. The emergence of *TP53* mutations as a key risk factor for stratification is evident given the significant adverse prognosis, even in the absence of del(17p)[6,8]. Moreover, *TP53* mutations in various cancers can lead to gain-of-function or dominant negative phenotypes, altering treatment response[9].

Functional *ex vivo* drug sensitivity testing of patients' tumor cells to hundreds of inhibitors can reveal cell dependencies and molecular vulnerabilities while accounting for patient variability[10–13]. Here we show that integration of drug sensitivity data with genomic, transcriptomic, and proteomic data from the same samples revealed a deeper functional view of the impact of *TP53* aberrations in CD138+ MM cells. The presence of *TP53* mutation associated with increased sensitivity to approved drugs, including conventional chemotherapeutics, irrespective of del(17p) status. In contrast, monoallelic *TP53* samples had a distinct molecular profile without a significant change in *ex vivo* drug responses. Overall, we explored novel therapeutic options for *TP53* aberrations in MM and identified vulnerabilities

61 associated with *TP53* mutation to multiple compounds, providing a foundation for targeted
62 treatment strategies to improve patient outcome.

63

64 **MATERIALS AND METHODS**

65 ***Patients and samples***

66 Bone marrow (BM) aspirates and skin biopsies were collected from patients under approved
67 protocols (239/13/03/00/2010 and 303/13/03/01/2011) in line with the Declaration of
68 Helsinki as previously described[10]. Following Ficoll (GE Healthcare) gradient separation of the
69 mononuclear cell fraction, CD138+ cells were enriched by immunomagnetic bead separation
70 (StemCell Technologies) and used for downstream assays. Interphase FISH was conducted
71 according to the European Myeloma Network 2012 guidelines[29]. Patient characteristics and
72 assays performed are detailed in **Table 1**.

73 ***Ex vivo drug screening and analysis***

74 Drug sensitivity testing was conducted using an established *ex vivo* drug screening method on
75 CD138+ cells, with viability measured by CellTiter-Glo reagent (Promega) after 72 hours[10–12].
76 BM CD138+ cells were added to pre-drugged plates, which contained up to 348 compounds
77 (**supplemental Table 1**). Quality control analysis, dose response curve fitting, and drug
78 sensitivity scores (DSS) were calculated as previously described[15].

79 ***Whole Exome Sequencing***

80 Genomic DNA was extracted from skin biopsies and CD138+ BM cells using the Qiagen DNeasy
81 Blood & Tissue kit or the Qiagen AllPrep DNA/RNA/miRNA Universal kit. The isolated DNA was
82 processed, exome libraries prepared and sequenced as described previously[11,31]. Somatic
83 mutations were identified and annotated using established methods[32]. The presence of a
84 mutation is considered if the variant frequency exceeded 5% (somatic p-value ≤ 0.05).

85 ***RNA Sequencing***

86 RNA from CD138+ cells isolated using the Qiagen AllPrep DNA/RNA/miRNA Universal kit,
87 RNAseq libraries were prepared using ribosome depletion, data pre-processing and the
88 analysis pipeline were carried out as described earlier[33]. Differential gene expression (DGE)
89 analysis was performed using DESeq2 R package (1.36.0)[34] from $\log_2$CPM raw counts
90 calculated with edgeR after TMM normalized. Within DESeq2, raw count data were filtered
91 to remove genes with less than 10 reads in at least 95% of the samples. For the gene set

92 enrichment analysis, we used clusterProfiler (4.4.4)[35] package and MSigDB (7.5.1) and from
93 that H (Hallmark) and C5 (GO) genesets, excluding human phenotype ontology sets (HPO)
94 [36,37].

95 ***Label-Free LC-MS/MS Analysis and Data Processing of CD138+ cells***

96 500 ng of each digested sample was analysed using Q-Exactive (ThermoFisher Scientific,
97 Hemel Hempstead, UK) high-resolution accurate mass spectrometer connected to a Dionex
98 Ultimate 3000 (RSLCnano) chromatography system (ThermoFisher Scientific, Hemel
99 Hempstead, UK). Peptides were separated and data acquired with MS/MS scans. Protein
100 identification and label-free quantification (LFQ) normalization were performed using
101 MaxQuant v1.5.2.8 (http://www.maxquant.org), with subsequent data analysis using
102 Perseus. In our figures, uniprot accession IDs are presented as gene symbol IDs. More details
103 are provided in the **supplemental Methods**.

104 ***Validation using public data***

105 We utilized the IA21 version of the MMRF-CoMMpass study (NCT01454297), available from
106 MMRF research gateway (https://research.themmrf.org/). Only CD138+ BM samples at
107 diagnosis were selected. The del(17p) status was determined using available seqFISH data[38].
108 DGE analysis was performed as described above. Survival analysis was performed in R using
109 survival (3.5-7)[39] and survminer (0.4.9)[40] packages.

110 ***Statistical Analyses***

111 Statistical analysis was done in R. Normality of the data was assessed using Shapiro-Wilk test
112 and based on the result either the Welch Two Sample t-test or Wilcoxon rank-sum test were
113 applied to subsequent analysis. Categorical data was analyzed using Fisher's exact test or chi-
114 square test according to the sample size. Kruskal-Wallis Test was applied to estimate the
115 difference between the age distribution of the groups. Resulted p-values were adjusted with
116 Benjamini-Hochberg. Survival analysis employed the Kaplan-Meier method and Cox
117 proportional hazards models.

118

119 **RESULTS**

120 ***Study sample characteristics***

121 Our study utilized data from 167 individuals receiving treatment throughout Finland.
122 Collected BM samples were processed for mononuclear cell selection and immunomagnetic

separation of CD138+ cells. DNA from the selected cells and a matching skin biopsy underwent whole exome sequencing to identify somatic mutations. Subsets of CD138+ cells were also used for bulk RNA sequencing and proteomic evaluation (**Figure 1A, B**). Additionally, the *ex vivo* sensitivity of the same CD138+ MM patient cells was assessed against an oncology drug collection of 348 small molecule inhibitors, with 153 total screened samples (**supplemental Table S1**). Other clinical data, such as karyotyping, was available and summarized information is provided in **Table 1**.

When focusing on *TP53* aberrations, the use of next-generation sequencing provides a more detailed view of the patient subpopulations as presented in the MMRF-CoMMpass cohort (**Figure 1C**). Characteristically, *TP53* mutation becomes more prevalent at relapse (15.2%) compared to diagnosis (7.2%). Given that mutated *TP53* leads to functional impairment of wild-type (WT) p53 protein[9,14], we grouped all samples with *TP53* mutation ($TP53^{mut/-}$ and $TP53^{mut/WT}$) in one category. This includes samples with additional detection of del(17p), also known as double-hit MM. Samples containing only wild-type copies of *TP53* but presented del(17p) from karyotyping are referred to as monoallelic *TP53* from here on. Five samples lacking sequencing results but with a detected del(17p) karyotype are also included in this category, for a total of 19 monoallelic *TP53* patient samples. The remaining samples (n = 130) were *TP53* WT.

Presence of TP53 mutation is associated with increased sensitivity to multiple drugs

In search of novel therapeutic vulnerabilities in high-risk patients harboring *TP53* aberrations, we analyzed data from our *ex vivo* drug screening platform. To measure the drug sensitivity of the samples, we used the drug sensitivity score (DSS), which is a modified version of the area under the curve. The DSS allows for comparison of dose-response curves across a range of concentrations, providing a single measure of the sensitivity of the cancer cells to the drug[15]**.** Confirming the difficulty to treat del(17p) patients, CD138+ MM cells with monoallelic *TP53* showed no significant increase in *ex vivo* sensitivity to the tested compounds. Conversely, samples with *TP53* mutation, regardless of the presence of del(17p), displayed higher sensitivity to certain mitotic inhibitors and inhibitors targeting RNA synthesis, HDAC, topoisomerase, HSP90, and the PI3K/AKT/mTOR pathway (**Figure 2A,B; supplemental Table S2**). The mutant p53 targeting compound APR-246 demonstrated enhanced activity in *TP53*

154 mutated MM, suggesting that it effectively reactivates the mutant p53 protein leading to cell
155 death. The biological significance of the specific grouping is also observed for monoallelic *TP53*
156 MM where increased resistance to the MDM2 antagonists idasanutlin (median difference = -
157 6.8; p-value = 0.074) and nutlin-3 (median difference = -2.6; p-value = 0.014) was observed.
158 Resistance to MDM2 antagonists suggests the reduced availability of p53 in samples with
159 monoallelic *TP53*, while the activity of APR-246 highlights the dominant effect of the mutant
160 p53 protein (**Figure 2C**). The impact of *TP53* mutation on *ex vivo* drug response is highlighted
161 by the comparison of DSS between *TP53* mutated and monoallelic *TP53* samples
162 (**supplemental Figure S1**).
163 The most remarkable increase in sensitivity of *TP53* mutated MM samples was observed for
164 plicamycin, an RNA synthesis inhibitor. The response to plicamycin was greater than that to
165 another RNA and DNA synthesis inhibitor, dactinomycin, which also showed a significant
166 increase in activity. Multiple conventional chemotherapeutics showed increased activity in
167 samples with *TP53* mutation, specifically mitotic inhibitors (vinorelbine, paclitaxel, docetaxel,
168 vincristine, ABT-751, patupilone) and topoisomerase inhibitors (teniposide, irinotecan,
169 daunarubicin, camptothecin, topotecan, etoposide, doxorubicin, idarubicin). Many
170 chemotherapeutics were tested on fewer samples, however, the consistency of the increased
171 sensitivity on similar compounds supports the observation that *TP53* mutated cells are more
172 sensitive to these drug classes (**supplemental Table S2**).
173 This increased activity was also evident with HDAC inhibitors quisinostat and panobinostat,
174 both approved treatments. In a smaller set of samples, CUDC-101, targeting class I/II HDAC
175 and EGFR also showed significantly increased activity in *TP53* mutated MM samples, while
176 belinostat showed increased, but not a significant difference in activity (median difference =
177 9.5; p-value = 0.072).
178 The heightened activity of PI3K/AKT/mTOR pathway inhibitors in *TP53* mutated MM CD138+
179 cells suggested a potential dependency on growth signals involving this pathway. We showed
180 increased *ex vivo* sensitivity to vistusertib, omipalisib, pictilisib, temsirolimus, and dactolisib.
181 Additionally, kinase inhibitors tirbanibulin, GSK-1904529A, BMS-754807, and ruxolitinib all
182 demonstrated increased activity in *TP53* mutated MM samples. GSK-1904529A and BMS-
183 754807 target IGF1-R and ruxolitinib specifically targets JAK1 and JAK2 kinases, which are
184 upstream of PI3K, AKT and mTOR. The HSP90 inhibitor tanespimycin, which indirectly

185 suppresses the PI3K/AKT/mTOR pathway[16], also showed significant increase in activity
186 towards *TP53* mutated CD138+ cells.
187 To assess the impact of *TP53* mutation frequency on the response to these compounds, we
188 correlated the response of each sample with the mutation frequency (**supplemental Figure**
189 **S2; supplemental Table S3**). To establish correlation, we selected compounds tested in at least
190 5 samples and highlighted compounds with significant difference observed in *TP53* mutated
191 MM (**supplemental Figure S2A)**. Except for JQ1, most compounds showed weak and non-
192 significant correlation to mutation frequency, probably owing to overall limited selective
193 toxicity of the compounds.
194
195 ***TP53 mutations frequently co-occur with KRAS mutations in MM***
196 To understand the broader genetic landscape of *TP53* aberrations in MM and search for
197 possible confounding factors in drug response, we explored the frequency of co-occurrence
198 of common mutations. In our cohort, almost half of the samples with *TP53* mutation also had
199 a mutation to *KRAS*, while *KRAS* mutations were rare in samples with monoallelic *TP53*
200 (Fisher's exact test: $p = 0.029$; OR = 6.44, 95% CI = [1.01, 73.93]; **Figure 3A**). However, *KRAS*
201 mutations were not more likely to be present in *TP53* mutated MM compared to MM with
202 WT *TP53* (Fisher's exact test: $p = 0.080$; OR = 0.378, 95% CI = [0.12, 1.21]). To assess whether
203 *TP53* and *KRAS* mutation co-occurrence is common in MM, we analyzed diagnostic samples
204 from the MMRF-CoMMpass study (**Figure 3B**). In this cohort, *KRAS* mutations were present in
205 14 out of 85 samples with *TP53* mutation (16.5% frequency), which was more common than
206 with WT *TP53* ($\chi^2 = 5.089$, df = 2, p-value = 0.024). To assess the impact of co-occurring *KRAS*
207 mutations on *ex vivo* drug response, we compared the drug sensitivity profiles of *TP53*
208 mutated MM with and without *KRAS* mutation. We found that samples with co-occurring
209 *TP53* and *KRAS* mutations were significantly more resistant to 5 compounds compared to
210 samples with mutated *TP53* and WT *KRAS* (**supplemental Figure S3**, **supplemental Table S4**).
211 *TP53* is often characterized by hotspot mutations, with the location of the mutation having
212 different functional impact on the resulting protein. Using the MMRF-CoMMpass dataset, we
213 found that most mutations in *TP53* were spread across the protein but occurred more
214 frequently in the DNA binding domain (**Figure 2C**). Similarly, in the FIMM cohort, most
215 mutations occurred in the DNA binding domain, with some samples containing more than one

216 mutation (**Table 2**). No other hotspot mutation was detected, in concordance with previous
217 observations in MM[17].
218

219 ***Differential gene expression analysis reveals a transcriptional profile of enhanced cellular***
220 ***proliferation in TP53 mutated MM***

221 To understand the cellular implications and functional impact of *TP53* mutations in MM, we
222 compared RNA sequencing data of *TP53* mutated to WT *TP53* MM samples and applied
223 differential gene expression (DGE) followed by gene set enrichment analysis (GSEA). To
224 explore the consistency of our analysis with a wider cohort, we followed the same steps using
225 data both from the FIMM cohort as well as the MMRF-CoMMpass study.
226 In the FIMM cohort, we compared 15 samples with *TP53* mutation against 77 WT *TP53*
227 samples, from which we identified 1043 differentially expressed genes (p-value $\leq$ 0.05), of
228 which 675 were upregulated and 368 downregulated (**Figure 4A**; **supplemental Tables S5-S7**).
229 From the CoMMpass study samples with RNA sequencing data available, we compared 52
230 samples exhibiting *TP53* mutation (8.6%) against 552 samples with WT *TP53*. This DGE analysis
231 provided 700 differentially expressed genes (adjusted p-value $\leq$ 0.01), of which 458 were
232 upregulated and 232 downregulated (**Figure 4B, supplemental Tables S8-S10**). The results
233 from both datasets were consistent and demonstrated that *TP53* mutated MM is associated
234 with cell proliferation gene expression signatures. The G2M checkpoint, E2F targets and
235 mitotic spindle formation were upregulated in both cohorts (**Figure 4C, D**). In addition to the
236 common findings, the CoMMpass dataset showed a significant upregulation of mTORC1
237 signaling and genes involved in glycolysis. On the other hand, the downregulation of gene sets
238 modulated by NF-κB in response to TNFalpha, hypoxia, response to interferon gamma, and
239 apoptosis were only significant in the FIMM cohort analysis.
240 Additionally, we explored the transcriptional impact of monoallelic *TP53* on both FIMM and
241 CoMMpass cohorts. DGE analysis of the FIMM cohort identified 724 differentially expressed
242 genes (p-value $\leq$ 0.05), of which 472 were upregulated and 252 downregulated (**supplemental**
243 **Figure S4A**). From the CoMMpass study samples, we identified 430 differentially expressed
244 genes (adjusted p-value $\leq$ 0.05), of which 230 were upregulated and 200 downregulated
245 (**supplemental Figure S4B**). GSEA revealed an increase in the G2M and E2F gene sets for

246 samples with monoallelic *TP53* only in the larger CoMMpass cohort (**supplemental Figure**
247 **S4C; supplemental Tables S11-S13**).
248
249 ***Proteomic profiling reveals elevated drug target expression in TP53 mutated MM***
250 To expand on our understanding of the functional molecular landscape associated with *TP53*
251 mutations in MM, we explored proteomic data produced by LC-MS/MS analysis of CD138+
252 cells from a subset of our samples. We performed proteomic analysis on 34 samples, of which
253 5 contained *TP53* mutation, 6 had monoallelic *TP53* and 23 were WT *TP53*. Out of the 2753
254 identified proteins, 430 exhibited significant difference between samples with *TP53* mutation
255 compared to WT *TP53* (Welch Two Sample t-test two sided; p-value $\leq$ 0.05; **Figure 5A**;
256 **supplemental Table S14**).
257 In alignment with the results from GSEA of RNA sequence data, we observed an enrichment
258 of E2F targets and G2M checkpoint proteins. Additionally, MYC targets were upregulated as
259 shown in **Figure 5B**. Analysis using the Gene Ontology (GO) C5 library revealed significant
260 enrichment of proteins associated with transcription processes, such as RNA binding,
261 RNA/mRNA processing, nuclear speckles, and RNA splicing (**Figure 5C**). Notably, the
262 ribonucleoprotein complex gene set, involved in ribosomal functions, including HURNPA3,
263 HNRNPA2B1, SNRPA1, and RNPS1, along with the FACT complex proteins SSRP1 and SUPT16H,
264 were highly expressed in the *TP53* mutated samples (**Figure 5A**; **supplemental Table**
265 **S14**).Among the gene sets enriched with the selected proteins, we observed downregulation
266 in the immune response and immune markers CD9, CD36 and CD76 suggesting a mechanism
267 of immune evasion. Other significantly downregulated gene sets included those associated
268 with mechanisms of adhesion and secretion. For the full list of gene sets enriched in this
269 analysis see **supplemental Tables S15-S16**.
270 Among the significantly expressed proteins identified, some are notable drug targets. We
271 observed increased expression of HDAC2, which is a target of HDAC inhibitors. This supports
272 the observed sensitivity to specific HDAC inhibitors, including the approved non-selective
273 inhibitors panobinostat and quisinostat, and the dual-acting inhibitor CUDC-101, which
274 targets both HDAC and EGFR pathways. Similarly, we observed significant upregulation of
275 HSP90AA1, the target of HSP90 inhibitor tanespimycin (**supplemental Figure S5;**
276 **supplemental Table S2**). While these single proteins can explain the efficacy of some targeted

277 compounds, the scope is limited by the specificity of the inhibitors and the detectable proteins
278 in our analysis.
279 In contrast, comparison of monoallelic *TP53* to WT *TP53* proteomic profiles exhibited 96
280 significantly expressed proteins, with 45 upregulated and 51 downregulated in the
281 monoallelic *TP53* samples. We observed an increase in gene sets related to protein transport
282 and a decrease in mitochondrial matrix and ribonucleoprotein complex (**supplemental Figure**
283 **S6; supplemental Tables S17-S18**).

284

285 ***Clinical Implications of TP53 aberrations***

286 To translate our findings to the clinic and evaluate the impact on prognosis of *TP53* mutations,
287 we leveraged the comprehensive dataset provided by the MMRF-CoMMpass study and
288 investigated the clinical prognosis of patients with or without *TP53* mutation.
289 A significant reduction in overall survival (OS) was notable among patients with *TP53*
290 mutation as compared to those with WT *TP53* (OS: HR = 2.004 [95% CI: 1.314-3.057] p = 0.001;
291 **Figure 5D**). Surprisingly, patients with monoallelic loss of *TP53* showed no significant
292 reduction in OS compared to patients with WT *TP53*, but they clearly had shorter progression
293 free survival (OS: HR = 1.264 [95% CI: 0.681-2.343] p = 0.458; PFS: HR = 1.356 [95% CI: 0.997-
294 1.846] p = 0.053; **Figure 5E**). Patients with monoallelic *TP53* had a median PFS of 530 days
295 (17.4 months) compared to 628 (20.6 months) for patients with *TP53* mutation. This suggests
296 that the presence of *TP53* mutation can lead to a more aggressive disease after the first
297 relapse, possibly because of clonal expansion. Although there is an increase in patients with
298 *TP53* mutation at relapse (**Figure 1**), due to lack of variant allele frequency data in the MMRF-
299 CoMMpass dataset we were not able to explore the clonal evolution of *TP53* mutations.

300

301 **DISCUSSION**

302 In our study we provide a comprehensive view and contribute significant insight into the
303 consequences of *TP53* aberrations in MM by applying a multi-omic approach to a large set of
304 patient samples. Functional assessment by *ex vivo* drug sensitivity testing along with genomic,
305 transcriptomic, and proteomic analyses highlight the biological impact of *TP53* mutations and
306 revealed potential treatment vulnerabilities. Notably, our findings discerned distinct
307 differences in *ex vivo* drug responses between MM with *TP53* mutation and MM with

308 monoallelic *TP53* when compared to samples with WT diploid *TP53*. These results were
309 further supported by differences in the genomic, transcriptomic, and proteomic landscapes of
310 these patients. Our research provides novel insights into the vulnerabilities of MM with *TP53*
311 mutations, with or without del(17p), as well as underscoring the need and suggesting
312 potential personalized therapeutic strategies for this high-risk subset of patients for future
313 investigations.
314 The clinical landscape of MM has long been influenced by the presence of del(17p), a well-
315 documented adverse prognostic factor[2]**.** With the advent of sequencing technologies, *TP53*
316 mutations have emerged as a novel prognosis marker in MM[6,17], yet their distinct functional
317 impact compared to del(17p) has not been fully recognized until now. Our study showed that
318 unlike monoallelic *TP53*, *TP53* mutations in CD138+ cells confer increased sensitivity to
319 multiple small molecule inhibitors. This finding presents opportunities to develop effective
320 treatment strategies that includes conventional chemotherapies and other approved drugs.
321 By focusing on patients with *TP53* mutation, we have the potential to mitigate the risk for
322 almost half of the del(17p) cases, including those with double-hit MM and those with *TP53*
323 mutation and intact chromosome 17. However, our results reaffirm the continued challenges
324 of treating del(17p) MM.
325 Drug sensitivity testing of MM samples from a large cohort of patients demonstrated that MM
326 with *TP53* mutation is vulnerable to multiple approved and investigational drugs with known
327 target profiles. Even at low variant allele frequency (VAF) CD138+ MM cells with a minimum
328 *TP53* mutation VAF of 5% displayed increased sensitivity to a spectrum of compounds,
329 including conventional chemotherapeutics, topoisomerase, RNA synthesis, HDAC, HSP90,
330 IGF1R and PI3K/AKT/mTOR pathway inhibitors. HSP90 and HDAC inhibitors have already been
331 described to have critical roles in the degradation of mutant *TP53* in other types of cancer[18].
332 The increased expression of proteins HSP90AA1 and HDAC2, together with the increased
333 sensitivity to HSP90 and HDAC inhibitors, suggest a critical role for these factors in *TP53*
334 mutated MM cell survival. *TP53* mutations have been previously reported to upregulate *IGF1R*
335 expression and IGF-1 mediated mitogenesis, possibly through reduced p53 levels and
336 increased demand for new ribosomes, leading to MDM2-p53 interaction[19,20]. Subsequent
337 mTOR pathway activation leads to increased cell proliferation, increased mRNA translation
338 and increased glycolytic activity[19–21]. The observed increase in expression of ribosomal

339 subunits, together with the enrichment of genes involved in glycolysis and mTORC1 signaling
340 may explain the enhanced vulnerability to IGF1R, PI3K/AKT/mTOR inhibitors.
341 Both gene expression and proteomic analyses showed enrichment of pathways associated
342 with increased cell proliferation in *TP53* mutated MM. Consequently, common
343 chemotherapies including mitotic inhibitors (i.e. paclitaxel and vincristine), intercalating
344 agents (i.e. doxorubicin and gemcitabine) and topoisomerase inhibitors (i.e. topotecan,
345 etoposide and idarubicin) showed increased activity in CD138+ cells with *TP53* mutation. In
346 contrast, CD138+ cells with monoallelic *TP53* did not display an increase in sensitivity to
347 chemotherapies when compared to cells from patients with WT *TP53*.
348 The enhanced sensitivity of *TP53* mutated samples to doxorubicin, plicamycin and
349 dactinomycin may be explained by their mechanisms of action and association with ribosomal
350 biogenesis and mRNA processing[22,23]. Proteomic analysis revealed that proteins belonging to
351 the ribonucleoprotein complex are upregulated in mutated *TP53* and downregulated in
352 monoallelic *TP53* MM. Doxorubicin has been previously shown to inhibit the synthesis of 47S
353 rRNA precursor[23], while it also acts as intercalator similarly to daunorubicin and idarubicin.
354 The RNA synthesis inhibitor plicamycin showed the largest difference in activity between *TP53*
355 mutated and WT *TP53* samples. Plicamycin selectively targets genes with GC-rich promoter
356 sequences, activates any remaining wild-type p53 and inhibits the transcriptional regulator
357 SP1 from DNA binding, including to the promoter of *TP53*[23]. The enrichment of pathways
358 associated with mRNA processing and chromatin modulation suggests altered transcriptional
359 regulation and DNA replication in *TP53* mutated MM, which is similar to findings in other
360 cancers[9,18,24,25].
361 When exploring potential confounding genomic factors that may contribute to the enhanced
362 drug sensitivity profile in *TP53* mutated MM cells, we noticed that *TP53* mutations were
363 frequently accompanied by *KRAS* mutations, which was not observed in monoallelic *TP53*
364 MM. However, when we compared the drug response profiles of samples with *TP53* mutation
365 and WT *KRAS* to samples with both *TP53* and *KRAS* mutation, we only found 5 drugs were
366 significantly affected by the presence of a *KRAS* mutation, with the *KRAS* mutation conferring
367 a slight negative effect on the activity of these drugs. These results indicate that mutation to
368 *TP53* is the main contributor to the enhanced drug sensitivity and altered transcriptomic and
369 proteomic profiles of *TP53* mutated cells. Further research is needed to understand the
370 mechanisms leading to enhanced sensitivity to drugs such as plicamycin and doxorubicin and

371 their impact on MM cells and disease models with mutated *TP53*. Additionally, other drugs
372 that were not included in our panel could be effective for patients with *TP53* mutation positive
373 MM. For example, our proteomic analysis showed elevated levels of XPO1, the target of
374 approved MM drug selinexor, and its cofactor RANBP3, which are exclusively responsible for
375 transporting p53 out of the nucleus[26,27]. Considering the enhanced activity of several
376 chemotherapies in *TP53* mutated CD138+ MM cells, newer agents such as the antibody-drug
377 conjugate blenrep and peptide-drug conjugate melflufen might also provide increased efficacy
378 for patients with *TP53* mutated MM. In addition, novel therapeutic approaches, such as CAR-
379 T cell therapies, bispecific and monoclonal antibodies have shown promising results for MM
380 in clinical settings[28]. Our drug screening, however, was limited to small molecules, which were
381 tested, depending on cell availability, on isolated CD138+ MM cells without the supporting
382 immune microenvironment. Nevertheless, the results revealed targetable vulnerabilities in
383 *TP53* mutated MM, which could be investigated further for future therapeutic development.
384 While our comprehensive profiling showed that mutation to *TP53* can impact *ex vivo* drug
385 response as well as the transcriptomic and proteomic profiles to cells with the mutation, we
386 have only recently gained understanding of the significance of this aberration on patient
387 outcome. The adverse effect of *TP53* mutation on overall survival suggests that early detection
388 of subclonal *TP53* mutations could potentially predict faster disease progression after relapse
389 and allow for earlier intervention. This would be particularly important for patients without
390 del(17p) but with mutated *TP53*, as these patients may not be correctly stratified and are less
391 likely to receive optimized care.
392 In conclusion, our study offers translational insights into the implications of *TP53* mutations in
393 MM. Our findings elucidate key molecular aspects from genomic to proteomic landscapes,
394 guiding future research and therapeutic strategies for this subgroup of patients. As the
395 complexities of MM continue to be unraveled with the application of advanced technologies,
396 we will gain better understanding of the impact of genetic mutations like *TP53*, and how these
397 can shape the future of MM risk-stratification and treatment. These findings emphasize the
398 importance of personalized medicine approaches in oncology and provide rationale for the
399 development of multiple therapeutic strategies and treatment of *TP53* mutated MM.
400
401 **FIGURE LEGENDS**

402 **Table 1.** Summarized characteristics of MM patients providing samples to the FIMM cohort
403 and the analyses performed.
404 **Table 2**. *TP53* mutations detected in patients from the FIMM dataset.
405 **Figure 1. Workflow and patient stratification according to *TP53* status.** (A) CD138+ cells from
406 167 bone marrow samples were molecularly and functionally profiled depending on viable
407 cell numbers. (B) Dataset used from the MMRF-CoMMpass study for validation purposes. (C)
408 Comparison of patient *TP53* status with and without DNA sequencing in the MMRF-
409 CoMMpass patient population. Remaining patient proportion in grey represents wild-type
410 (WT) *TP53* status.
411 **Figure 2. *Ex vivo* drug screening identifies compounds with enhanced activity in MM patient**
412 **samples with *TP53* mutation.** (A) Volcano plot illustrating the comparison of drug sensitivity
413 between MM samples with monoallelic *TP53* and WT *TP53* samples. No compounds
414 presented significantly increased sensitivity for samples with monoallelic *TP53*. (B) Samples
415 harboring *TP53* mutations, irrespective of del(17p) status, exhibit increased sensitivity to a
416 range of therapeutic agents. The volcano plot's x-axis shows the median difference in DSS
417 between the two groups, while the y-axis represents the negative logarithm (base10) of the
418 p-value obtained from the Wilcoxon rank-sum test. Data points represent individual
419 compounds, with the datapoint size reflecting the number of samples tested per compound.
420 Significant hits with median difference above 5 are highlighted in red, and a few additional
421 selected compounds are also labeled but remain in grey. (C) Box plot showing the distribution
422 of *ex vivo* sensitivity to selected compounds. DSS below 10 indicates overall resistance to the
423 compounds. The center line represents the median value. The upper and lower limits of the
424 box represent the upper (75th percentile) and lower (25th percentile) quartiles, respectively.
425 The whiskers extend to the largest and smallest values within 1.5 times the interquartile range
426 from the quartiles. Points beyond the whiskers are outliers and are plotted individually.
427 Statistical significance indicated as * p-value < 0.05, ** p-value < 0.01, *** p-value < 0.001 by
428 Wilcoxon rank-sum test.
429 **Figure 3. Co-occurrence of other mutations in addition to *TP53* aberrations.** (A) Heatmap of
430 common mutations in samples with *TP53* aberrations from the FIMM cohort. *KRAS* mutations
431 in samples with *TP53* mutation are overrepresented compared to del(17p) alone. (B) Heatmap
432 of common mutations in patients containing *TP53* aberrations from the MMRF-CoMMpass
433 study dataset. (C) Frequency of mutations in the *TP53* coding region from 52 patients of the

434 MMRF-CoMMpass study according to available data. The illustration of the functional
435 domains in the p53 protein includes the transcriptional activation domains (TAD, in blue and
436 green), the DNA binding domain (DBD, in red) and the tetramerization domain (TD, in orange).
437 **Figure 4. Genes sets associated with cellular proliferation are enriched in TP53 mutated MM.**
438 (A) Differential gene expression (DGE) in *TP53* mutated MM samples compared to WT *TP53*
439 samples from the FIMM dataset. The x-axis shows the log2 fold change in expression and the
440 y-axis shows the negative log10 of the p-value. Red dots represent genes with increased
441 expression in *TP53* mutated MM, while decreased expression is represented with blue dots.
442 (B) DGE analysis from the CoMMpass dataset, represented similarly, however the y-axis shows
443 the negative log10 of the adjusted p-value. (C) Gene set enrichment analysis (GSEA) results
444 compared between both datasets, ordered by normalized enrichment score (NES) of the
445 FIMM dataset. The gene sets shown have an adjusted p-value ≤ 0.1 in at least one of the two
446 datasets. (D) GSEA network plot illustrating the relationship between differentially expressed
447 genes from selected hallmark gene sets. The genes shown are differentially expressed in
448 CoMMpass dataset.
449 **Figure 5. Proteins involved in RNA processing are more prevalent in *TP53* mutated MM cells.**
450 (A) Significantly increased expression of proteins from samples with *TP53* mutation compared
451 to WT *TP53* samples is represented in a volcano plot. The x-axis shows the difference in the
452 mean level of protein expression, with the y-axis representing negative log10 of the p-value.
453 Red dots represent genes with increased expression in *TP53* mutated MM, while decreased
454 expression is represented with blue dots. (B) GSEA of significant proteins on the hallmarks
455 database reaffirm the results from the gene expression analysis, which showed gene sets
456 associated with increased proliferation are enriched in *TP53* mutated MM. (C) The ten most
457 positively and five most negatively enriched gene sets on GO C5 database. Gene sets are
458 presented in descending order of normalized enrichment score (NES). (D) Analysis shows
459 significant reduction in survival for patients with *TP53* mutation compared to WT *TP53* (OS:
460 2.004 [95% CI: 1.314-3.057] p = 0.001). Monoallelic loss of *TP53* (cut-off ≥ 20%) suggests a
461 comparatively better prognosis (OS: HR = 1.264 [95% CI: 0.681-2.343] p = 0.458). (E)
462 Monoallelic loss of *TP53*, with presence of WT *TP53* shows short progression free survival
463 (PFS) of 530 days (PFS: HR = 1.356 [95% CI: 0.997-1.846] p = 0.053). On the other hand,
464 presence of *TP53* mutation shows a delayed median progression 628 days (PFS: HR = 1.024
465 [95% CI: 0.832-1.260] p = 0.823), WT patients' median PFS was 689 days.

ACKNOWLEDGMENTS

The authors thank the patients for their consent and generosity to use their samples and data. We are grateful for the support of the FIMM Technology Center Genomics and High Throughput Biomedicine Units. In addition, we thank the Multiple Myeloma Research Foundation (MMRF) for making their datasets publicly available. The Finnish Hematology Registry and Biobank and the Helsinki Hematology Research Unit are acknowledged for contributions to the sample collection and clinical data.

AUTHOR CONTRIBUTIONS

C.A.H., D.T., and M.M.M. contributed to the study conceptualization. D.T., J.M., A.P., M.S., and M.M.M. performed experimental work. S.E. performed data normalizations for proteomic and sequencing data. K.D., P.D., D.B. and P.O'G. performed LC-MS/MS experiments and contributed to proteomics data analysis. D.T. performed data analysis and interpretation with N.I.'s contribution. J.L., R.S. and P.A. provided patient samples and contributed clinical data. D.T., J.J.M., I.V., N.I. and C.A.H. contributed to data management. D.T. and C.A.H. wrote the article. C.A.H. supervised the study and provided infrastructure support. All authors critically read and approved the final version of the article.

CONFLICTS OF INTEREST

C.A.H has received funding from BMS/Celgene, Kronos Bio, Novartis, Oncopeptides, WNTResearch, and Zentalis Pharmaceuticals for research unrelated to this work, and honorarium from Amgen and Autolus. R.S. has received research funding from Amgen, BMS/Celgene and Takeda administered by Hospital Science Centers, unrelated to this work. All other authors declare no conflicts of interest.

REFERENCES

1. Gulla A, Anderson KC. Multiple myeloma: the (r)evolution of current therapy and a glance into future. *Haematologica*. 2020;105(10):2358–2367.

495 2. Wiedmeier-Nutor JE, Bergsagel PL. Review of Multiple Myeloma Genetics including
496 Effects on Prognosis, Response to Treatment, and Diagnostic Workup. *Life (Basel)*.
497 2022;12(6):812.
498 3. Corre J, Perrot A, Caillot D, et al. del(17p) without TP53 mutation confers a poor
499 prognosis in intensively treated newly diagnosed patients with multiple myeloma. *Blood*.
500 2021;137(9):1192–1195.
501 4. Chavan SS, He J, Tytarenko R, et al. Bi-allelic inactivation is more prevalent at relapse in
502 multiple myeloma, identifying RB1 as an independent prognostic marker. *Blood Cancer J*.
503 2017;7(2):e535.
504 5. Walker BA, Mavrommatis K, Wardell CP, et al. A high-risk, Double-Hit, group of newly
505 diagnosed myeloma identified by genomic analysis. *Leukemia*. 2019;33(1):159–170.
506 6. Flynt E, Bisht K, Sridharan V, et al. Prognosis, Biology, and Targeting of TP53
507 Dysregulation in Multiple Myeloma. *Cells*. 2020;9(2):287.
508 7. Weinhold N, Ashby C, Rasche L, et al. Clonal selection and double-hit events involving
509 tumor suppressor genes underlie relapse in myeloma. *Blood*. 2016;128(13):1735–1744.
510 8. Corre J, Munshi NC, Avet-Loiseau H. Risk factors in multiple myeloma: is it time for a
511 revision? *Blood*. 2021;137(1):16–19.
512 9. Chen X, Zhang T, Su W, et al. Mutant p53 in cancer: from molecular mechanism to
513 therapeutic modulation. *Cell Death Dis*. 2022;13(11):1–14.
514 10. Majumder MM, Silvennoinen R, Anttila P, et al. Identification of precision treatment
515 strategies for relapsed/ refractory multiple myeloma by functional drug sensitivity
516 testing. *Oncotarget*. 2017;8(34):56338–56350.
517 11. Malani D, Kumar A, Brück O, et al. Implementing a Functional Precision Medicine Tumor
518 Board for Acute Myeloid Leukemia. *Cancer Discov*. 2022;12(2):388–401.
519 12. Kuusanmäki H, Kytölä S, Vänttinen I, et al. *Ex vivo* venetoclax sensitivity testing predicts
520 treatment response in acute myeloid leukemia. *Haematologica*. 2023;108(7):1768–1781.
521 13. Kropivsek K, Kachel P, Goetze S, et al. Ex vivo drug response heterogeneity reveals
522 personalized therapeutic strategies for patients with multiple myeloma. *Nat Cancer*.
523 2023;4(5):734–753.
524 14. Gencel-Augusto J, Lozano G. p53 tetramerization: at the center of the dominant-negative
525 effect of mutant p53. *Genes Dev.* 2020;34(17–18):1128–1146.

526 15. Yadav B, Pemovska T, Szwajda A, et al. Quantitative scoring of differential drug sensitivity
527 for individually optimized anticancer therapies. *Sci Rep*. 2014;4(1):5193.
528 16. Richardson PG, Mitsiades CS, Laubach JP, et al. Inhibition of heat shock protein 90
529 (HSP90) as a therapeutic strategy for the treatment of myeloma and other cancers.
530 *British Journal of Haematology*. 2011;152(4):367–379.
531 17. Martello M, Poletti A, Borsi E, et al. Clonal and subclonal TP53 molecular impairment is
532 associated with prognosis and progression in multiple myeloma. *Blood Cancer J.*
533 2022;12(1):15.
534 18. Hu J, Cao J, Topatana W, et al. Targeting mutant p53 for cancer therapy: direct and
535 indirect strategies. *Journal of Hematology & Oncology*. 2021;14(1):157.
536 19. Lindström MS, Bartek J, Maya-Mendoza A. p53 at the crossroad of DNA replication and
537 ribosome biogenesis stress pathways. *Cell Death Differ*. 2022;29(5):972–982.
538 20. Werner H, LeRoith D. Hallmarks of cancer: The insulin-like growth factors perspective.
539 *Front. Oncol.* 2022;12:1055589.
540 21. Cui D, Qu R, Liu D, et al. The Cross Talk Between p53 and mTOR Pathways in Response to
541 Physiological and Genotoxic Stresses. *Front. Cell Dev. Biol.* 2021;9:775507.
542 22. Kang J, Brajanovski N, Chan KT, et al. Ribosomal proteins and human diseases: molecular
543 mechanisms and targeted therapy. *Sig Transduct Target Ther*. 2021;6(1):1–22.
544 23. Burger K, Mühl B, Harasim T, et al. Chemotherapeutic drugs inhibit ribosome biogenesis
545 at various levels. *J Biol Chem*. 2010;285(16):12416–12425.
546 24. Bhakat KK, Ray S. The FAcilitates Chromatin Transcription (FACT) complex: Its roles in
547 DNA repair and implications for cancer therapy. *DNA Repair*. 2022;109:103246.
548 25. Zhu J, Sammons MA, Donahue G, et al. Gain-of-function p53 mutants co-opt chromatin
549 pathways to drive cancer growth. *Nature*. 2015;525(7568):206–211.
550 26. Golomb L, Bublik DR, Wilder S, et al. Importin 7 and exportin 1 link c-Myc and p53 to
551 regulation of ribosomal biogenesis. *Mol Cell*. 2012;45(2):222–232.
552 27. Azmi AS, Uddin MH, Mohammad RM. The nuclear export protein XPO1 — from biology
553 to targeted therapy. *Nat Rev Clin Oncol*. 2021;18(3):152–169.
554 28. Rasche L, Hudecek M, Einsele H. CAR T-cell therapy in multiple myeloma: mission
555 accomplished? *Blood*. 2024;143(4):305–310.

556 29. Ross FM, Avet-Loiseau H, Ameye G, et al. Report from the European Myeloma Network
557 on interphase FISH in multiple myeloma and related disorders. *Haematologica*.
558 2012;97(8):1272–1277.
559 30. Karjalainen R, Pemovska T, Popa M, et al. JAK1/2 and BCL2 inhibitors synergize to
560 counteract bone marrow stromal cell–induced protection of AML. *Blood*.
561 2017;130(6):789–802.
562 31. Kontro M, Kuusanmäki H, Eldfors S, et al. Novel activating STAT5B mutations as putative
563 drivers of T-cell acute lymphoblastic leukemia. *Leukemia*. 2014;28(8):1738–1742.
564 32. Eldfors S, Kuusanmäki H, Kontro M, et al. Idelalisib sensitivity and mechanisms of disease
565 progression in relapsed TCF3-PBX1 acute lymphoblastic leukemia. *Leukemia*.
566 2017;31(1):51–57.
567 33. Kumar A, Kankainen M, Parsons A, et al. The impact of RNA sequence library
568 construction protocols on transcriptomic profiling of leukemia. *BMC Genomics*.
569 2017;18(1):629.
570 34. Love MI, Huber W, Anders S. Moderated estimation of fold change and dispersion for
571 RNA-seq data with DESeq2. *Genome Biology*. 2014;15(12):550.
572 35. Wu T, Hu E, Xu S, et al. clusterProfiler 4.0: A universal enrichment tool for interpreting
573 omics data. *Innovation*. 2021;2(3):.
574 36. Subramanian A, Tamayo P, Mootha VK, et al. Gene set enrichment analysis: A
575 knowledge-based approach for interpreting genome-wide expression profiles.
576 *Proceedings of the National Academy of Sciences*. 2005;102(43):15545–15550.
577 37. Liberzon A, Subramanian A, Pinchback R, et al. Molecular signatures database (MSigDB)
578 3.0. *Bioinformatics*. 2011;27(12):1739–1740.
579 38. Goldsmith SR, Fiala MA, Dukeman J, et al. Next Generation Sequencing-based Validation
580 of the Revised International Staging System for Multiple Myeloma: An Analysis of the
581 MMRF CoMMpass Study. *Clinical Lymphoma Myeloma and Leukemia*. 2019;19(5):285–
582 289.
583 39. Therneau T. A package for survival analysis in R. 2020;
584 40. Kassambara A, Kosinski M, Biecek P, Fabian S. survminer: Drawing Survival Curves using
585 "ggplot2." 2021;

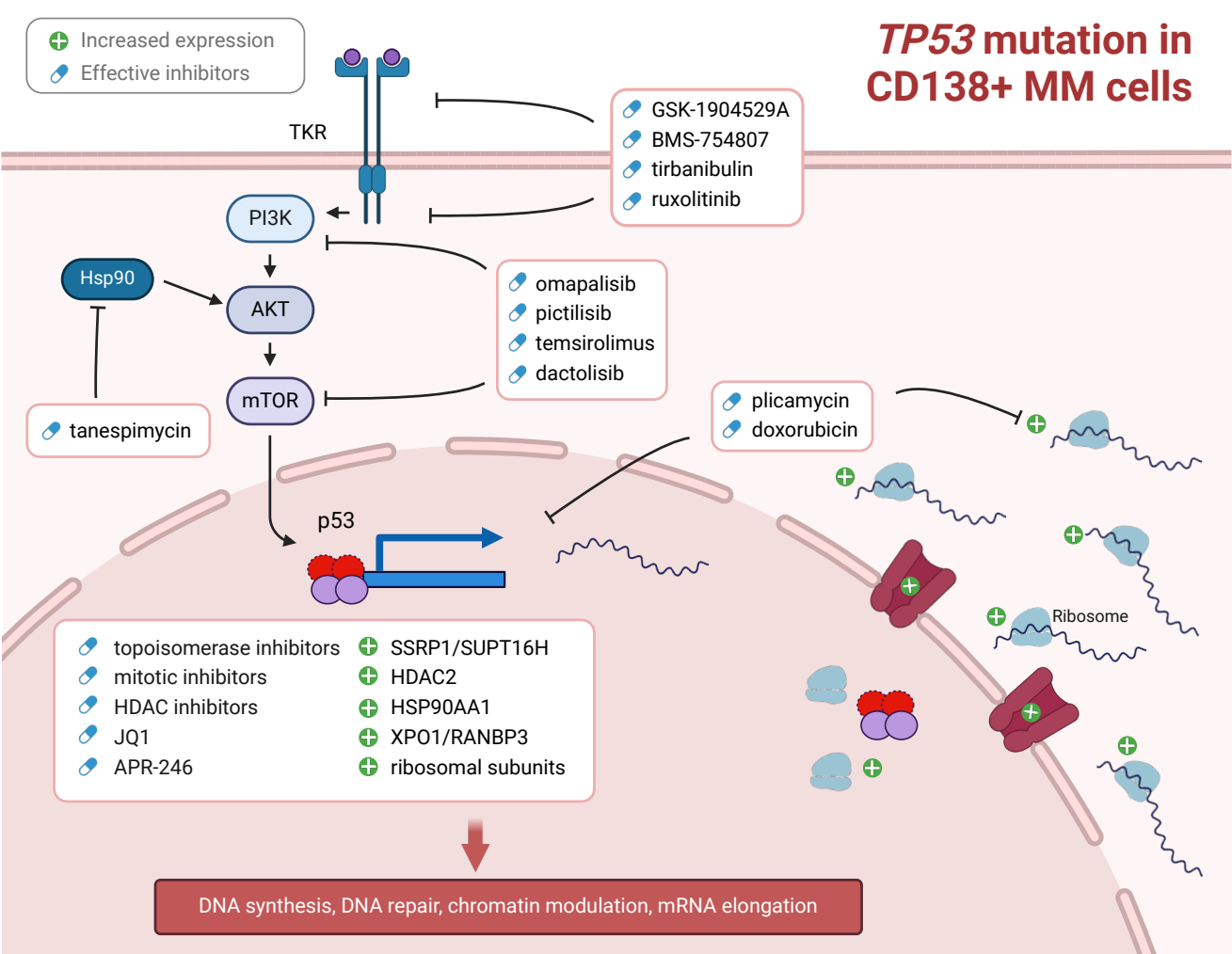
Increased expression
Effective inhibitors
TP53 mutation in CD138+ MM cells
TKR
GSK-1904529A
BMS-754807
tirbanibulin
ruxolitinib
PI3K
Hsp90
AKT
mTOR
omapalisib
pictilisib
temsirolimus
dactolisib
tanespimycin
plicamycin
doxorubicin
p53
Ribosome
topoisomerase inhibitors
mitotic inhibitors
HDAC inhibitors
JQ1
APR-246
SSRP1/SUPT16H
HDAC2
HSP90AA1
XPO1/RANBP3
ribosomal subunits
DNA synthesis, DNA repair, chromatin modulation, mRNA elongation

Table 1. Summarized characteristics of MM patients providing samples to the FIMM cohort and the analyses performed.

		Total (n = 167)	Monoallelic *TP53* (n = 19; 11.4%)	*TP53* mutation (n = 18; 10.8%)	WT *TP53* (n = 130; 77.8%)	*P* value
Median age (range)		67 (26-84)	67 (49-80)	67,5 (57-78)	66 (26-84)	0.921
Gender						0.103
	Male, n (%)	97 (58.1)	7 (36.8)	14 (77.8)	76 (58.5)	
	Female, n (%)	70 (41.9)	12 (63.2)	4 (22.2)	54 (41.5)	
Disease stage						0.006
	Diagnosis, n (%)	69 (41.3)	4 (21.1)	3 (16.7)	62 (47.7)	
	Relapse, n (%)	98 (58.7)	15 (78.9)	15 (83.3)	68 (52.3)	
Cytogenetics						
	del(17p), n (%)	26 (15.6)	19 (100)	7 (38.9)	0 (0.0)	0
	t(11;14), n (%)	30 (18.0)	2 (10.5)	2 (11.1)	26 (20.0)	0.556
	t(4;14), n (%)	16 (9.6)	4 (21.1)	0 (0.0)	12 (9.2)	0.081
	t(14;16), n (%)	2 (1.2)	1 (5.3)	0 (0.0)	1 (0.8)	0.395
	del(13q)/-13, n (%)	57 (34.1)	14 (73.7)	4 (22.2)	39 (30.0)	0.001
	1q gain, n (%)	57 (34.1)	12 (63.2)	6 (33.3)	39 (30.0)	0.017
	Not available, n (%)	41 (24.6)	0 (0.0)	5 (27.8)	36 (27.7)	0.014
Ex vivo drug screening		153 (91.6)	18 (94.7)	15 (78.9)	120 (92.3)	0.27
DNA sequencing, n (%)		135 (80.8)	14 (73.6)	18 (100)	103 (79.2)	0.052
RNA sequencing, n (%)		98 (58.7)	6 (31.6)	15 (83.3)	77 (59.2)	0.005
Proteomics, n (%)		34 (20.4)	6 (31.6)	5 (27.7)	23 (17.7)	0.265

Table 2. *TP53* mutations detected in patients from the FIMM dataset

Sample ID	Disease stage	del(17p)	Mutation Frequency in Tumor	Somatic P-Value	Chromosome Location	Base Change	Amino Acid Change	Variant Effect	Protein Domain
MM005_2	Relapse	Yes	0.2222	0.041812	Chr17:7572961	A>G	L383P	non synonymous coding	Regulatory Domain
MM007_1	Relapse	No	0.3359	1.2718e-14	Chr17:7577534	C>A	R249S	non synonymous coding	DNA-Binding Domain
MM010_1	Relapse	Yes	0.86	8.4891e-24	Chr17:7578185	GC>G	-221	frame shift	
MM025_1	Relapse	Yes	0.4175	3.5168e-17	Chr17:7577574	T>C	Y236C	non synonymous coding	DNA-Binding Domain
MM033_4	Relapse	Yes	0.2087	2.591e-05	Chr17:7578371	C>G	G187R	non synonymous coding	DNA-Binding Domain
MM041_1	Relapse	Yes	0.5833	6.9734e-07	Chr17:7577518	TGATGGTGAG>T	LTI252-	codon deletion	
MM042_1	Relapse	Yes	0.7536	1.2896e-12	Chr17:7577535	C>A	R249M	non synonymous coding	DNA-Binding Domain
MM043_2	Relapse	Yes	0.7857	4.8947e-29	Chr17:7578242	C>G	V203L	non synonymous coding	DNA-Binding Domain
MM043_2	Relapse	Yes	0.125	0.0034623	Chr17:7578204	A>C	S215R	non synonymous coding	DNA-Binding Domain
MM055_1	Relapse	No	0.6436	1.7451e-24	Chr17:7578440	T>C	K164E	non synonymous coding	DNA-Binding Domain
MM060_2	Relapse	No	0.1314	0.00056092	Chr17:7577538	C>T	R248Q	non synonymous coding	DNA-Binding Domain
MM064_1	Diagnosis	No	0.4667	1.0176e-05	Chr17:7578190	T>C	Y220C	non synonymous coding	DNA-Binding Domain
MM064_1	Diagnosis	No	0.434	0.00016009	Chr17:7578176	C>A		splice site donor	
MM065_1	Diagnosis	Yes	0.1296	0.0016255	Chr17:7577022	G>A	R306*	stop gained	DNA-Binding Domain
MM085_2	Relapse	No	0.3265	1.0205e-06	Chr17:7574034	C>G	c.994-1G>C	splice acceptor variant+intron variant	
MM098_1	Relapse	Yes	0.623	1.9092e-17	Chr17:7578291	T>C		splice site acceptor	DNA-Binding Domain
MM107_1	Relapse	Yes	0.6579	9.7397e-14	Chr17:7579529	C>T	p.Trp53*/c.158G>A	stop gained	DNA-Binding Domain
MM122_1	Diagnosis	No	0.0929	0.011409	Chr17:7578433	G>T	S166*	stop gained	DNA-Binding Domain
MM135_1	Relapse	Yes	0.9478	3.7734e-39	Chr17:7578479	G>T	P151T	non synonymous coding	DNA-Binding Domain
MM137_1	Relapse	No	0.3817	9.5371e-10	Chr17:7577506	C>G	D259H	non synonymous coding	DNA-Binding Domain

Figure 1

A

FIMM dataset

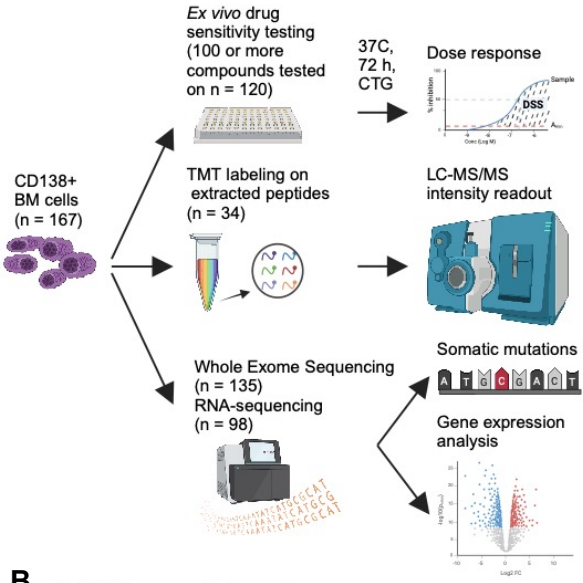

B

CoMMpass dataset

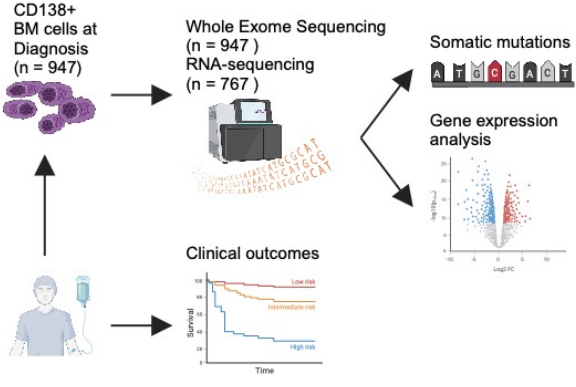

C

Only FISH available

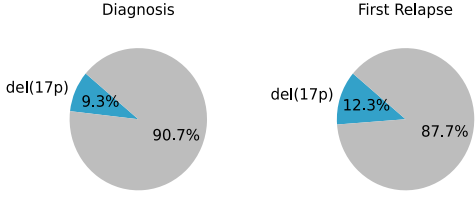

DNA sequencing available

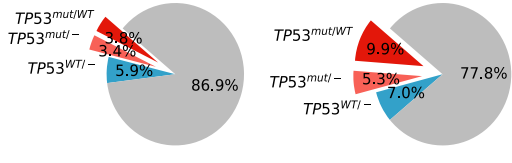

Figure 2

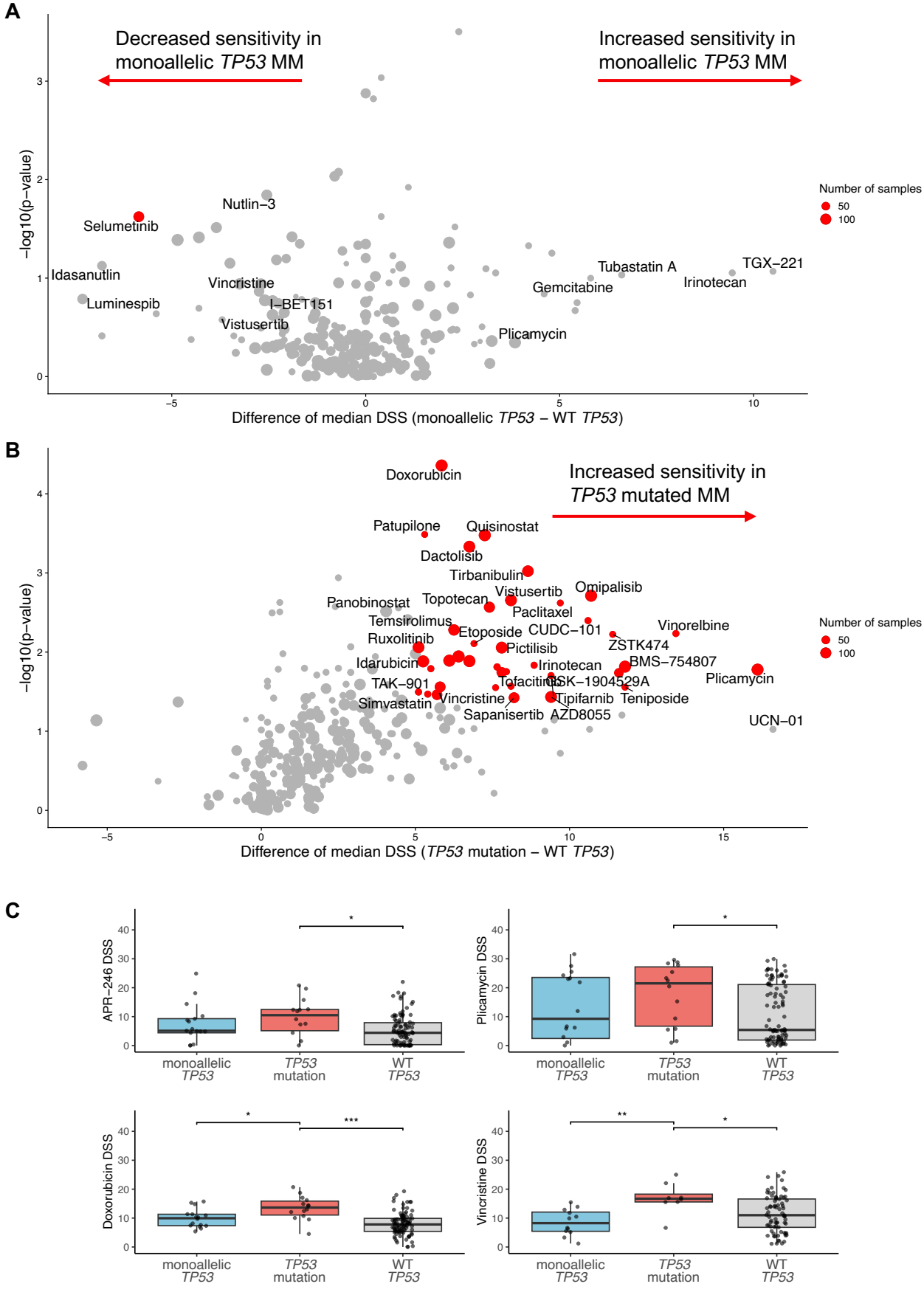
A
Decreased sensitivity in monoallelic TP53 MM
Increased sensitivity in monoallelic TP53 MM
−log10(p−value)
Difference of median DSS (monoallelic TP53 − WT TP53)
Number of samples
50
100
Selumetinib
Nutlin−3
Idasanutlin
Luminespib
Vincristine
I−BET151
Vistusertib
Plicamycin
Gemcitabine
Tubastatin A
Irinotecan
TGX−221
B
Increased sensitivity in TP53 mutated MM
−log10(p−value)
Difference of median DSS (TP53 mutation − WT TP53)
Number of samples
50
100
Doxorubicin
Patupilone
Quisinostat
Dactolisib
Tirbanibulin
Vistusertib
Omipalisib
Panobinostat
Topotecan
Paclitaxel
Temsirolimus
Etoposide
CUDC−101
Vinorelbine
Ruxolitinib
Pictilisib
ZSTK474
Idarubicin
Irinotecan
BMS−754807
TAK−901
Tofacitinib
GSK−1904529A
Plicamycin
Simvastatin
Vincristine
Tipifarnib
Teniposide
Sapanisertib
AZD8055
UCN−01
C
APR−246 DSS
Plicamycin DSS
Doxorubicin DSS
Vincristine DSS
monoallelic TP53
TP53 mutation
WT TP53

Figure 3

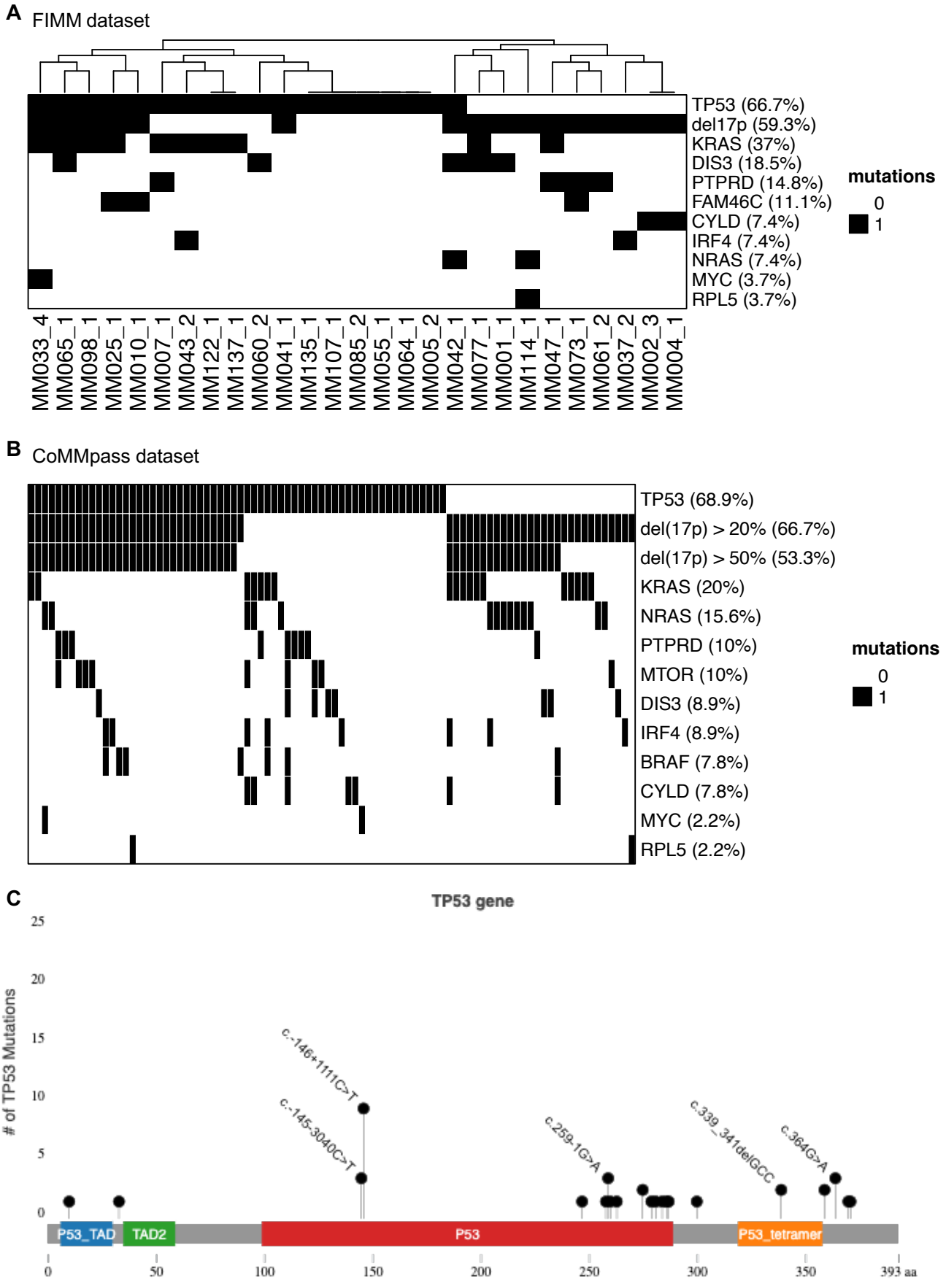
A
FIMM dataset
TP53 (66.7%)
del17p (59.3%)
KRAS (37%)
DIS3 (18.5%)
PTPRD (14.8%)
FAM46C (11.1%)
CYLD (7.4%)
IRF4 (7.4%)
NRAS (7.4%)
MYC (3.7%)
RPL5 (3.7%)
mutations
0
1
MM033_4
MM065_1
MM098_1
MM025_1
MM010_1
MM007_1
MM043_2
MM122_1
MM137_1
MM060_2
MM041_1
MM135_1
MM107_1
MM085_2
MM055_1
MM064_1
MM005_2
MM042_1
MM077_1
MM001_1
MM114_1
MM047_1
MM073_1
MM061_2
MM037_2
MM002_3
MM004_1
B
CoMMpass dataset
TP53 (68.9%)
del(17p) > 20% (66.7%)
del(17p) > 50% (53.3%)
KRAS (20%)
NRAS (15.6%)
PTPRD (10%)
MTOR (10%)
DIS3 (8.9%)
IRF4 (8.9%)
BRAF (7.8%)
CYLD (7.8%)
MYC (2.2%)
RPL5 (2.2%)
mutations
0
1
C
TP53 gene
# of TP53 Mutations
25
20
15
10
5
0
c.-146+1111C>T
c.-145-3040C>T
c.259-1G>A
c.339_341delGCC
c.364G>A
P53_TAD
TAD2
P53
P53_tetramer
0
50
100
150
200
250
300
350
393 aa

Figure 4

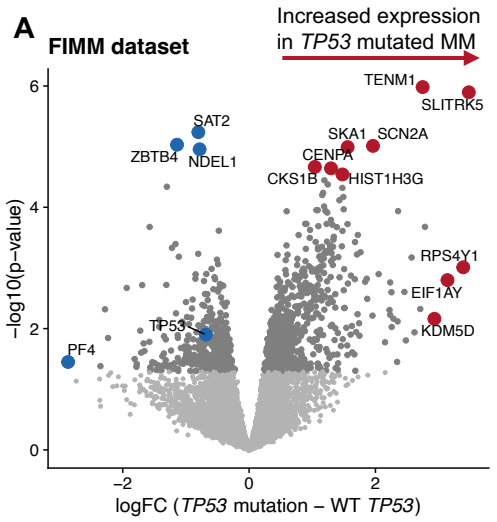
A
FIMM dataset
Increased expression in TP53 mutated MM
TENM1
SLITRK5
SAT2
ZBTB4
NDEL1
SKA1
SCN2A
CENPA
CKS1B
HIST1H3G
RPS4Y1
EIF1AY
KDM5D
TP53
PF4
−log10(p−value)
logFC (TP53 mutation – WT TP53)

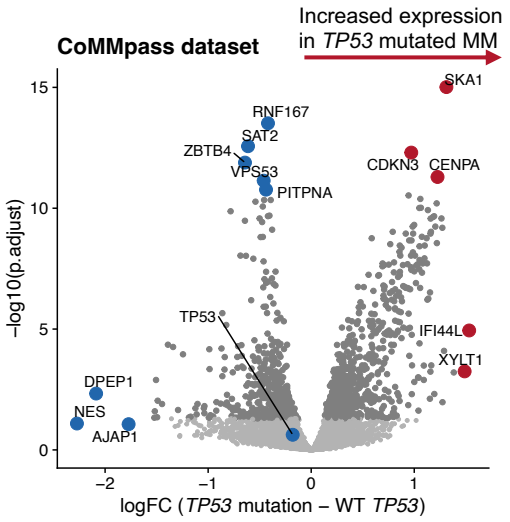
B
CoMMpass dataset
Increased expression in TP53 mutated MM
SKA1
RNF167
SAT2
ZBTB4
VPS53
PITPNA
CDKN3
CENPA
TP53
IFI44L
XYLT1
DPEP1
NES
AJAP1
−log10(p.adjust)
logFC (TP53 mutation – WT TP53)

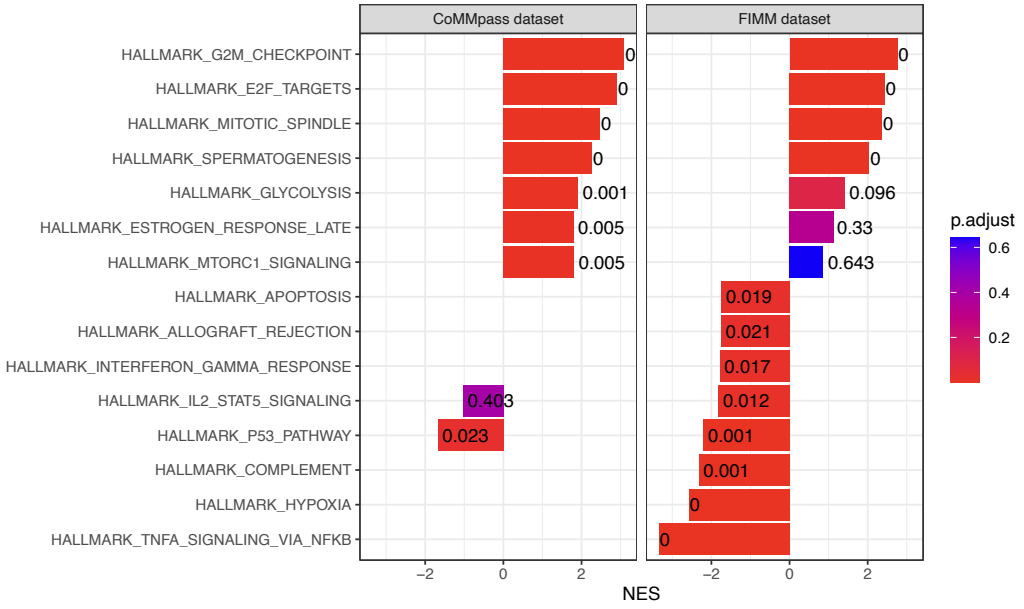
C
CoMMpass dataset
FIMM dataset
HALLMARK_G2M_CHECKPOINT
HALLMARK_E2F_TARGETS
HALLMARK_MITOTIC_SPINDLE
HALLMARK_SPERMATOGENESIS
HALLMARK_GLYCOLYSIS
HALLMARK_ESTROGEN_RESPONSE_LATE
HALLMARK_MTORC1_SIGNALING
HALLMARK_APOPTOSIS
HALLMARK_ALLOGRAFT_REJECTION
HALLMARK_INTERFERON_GAMMA_RESPONSE
HALLMARK_IL2_STAT5_SIGNALING
HALLMARK_P53_PATHWAY
HALLMARK_COMPLEMENT
HALLMARK_HYPOXIA
HALLMARK_TNFA_SIGNALING_VIA_NFKB
p.adjust
NES

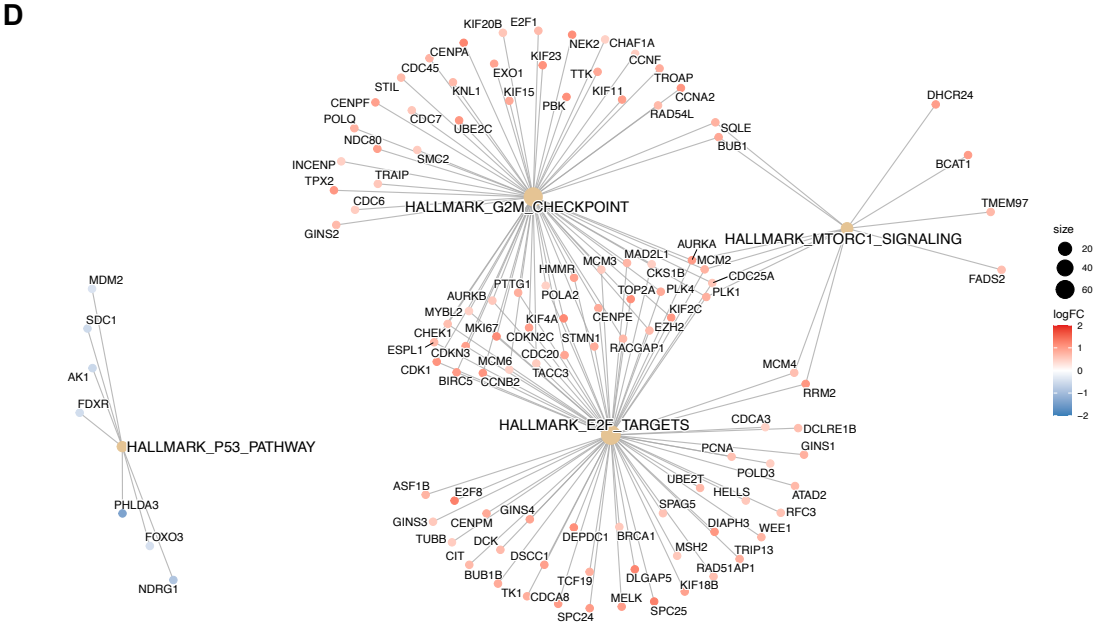
D
HALLMARK_G2M_CHECKPOINT
HALLMARK_MTORC1_SIGNALING
HALLMARK_E2F_TARGETS
HALLMARK_P53_PATHWAY
size
logFC

Figure 5

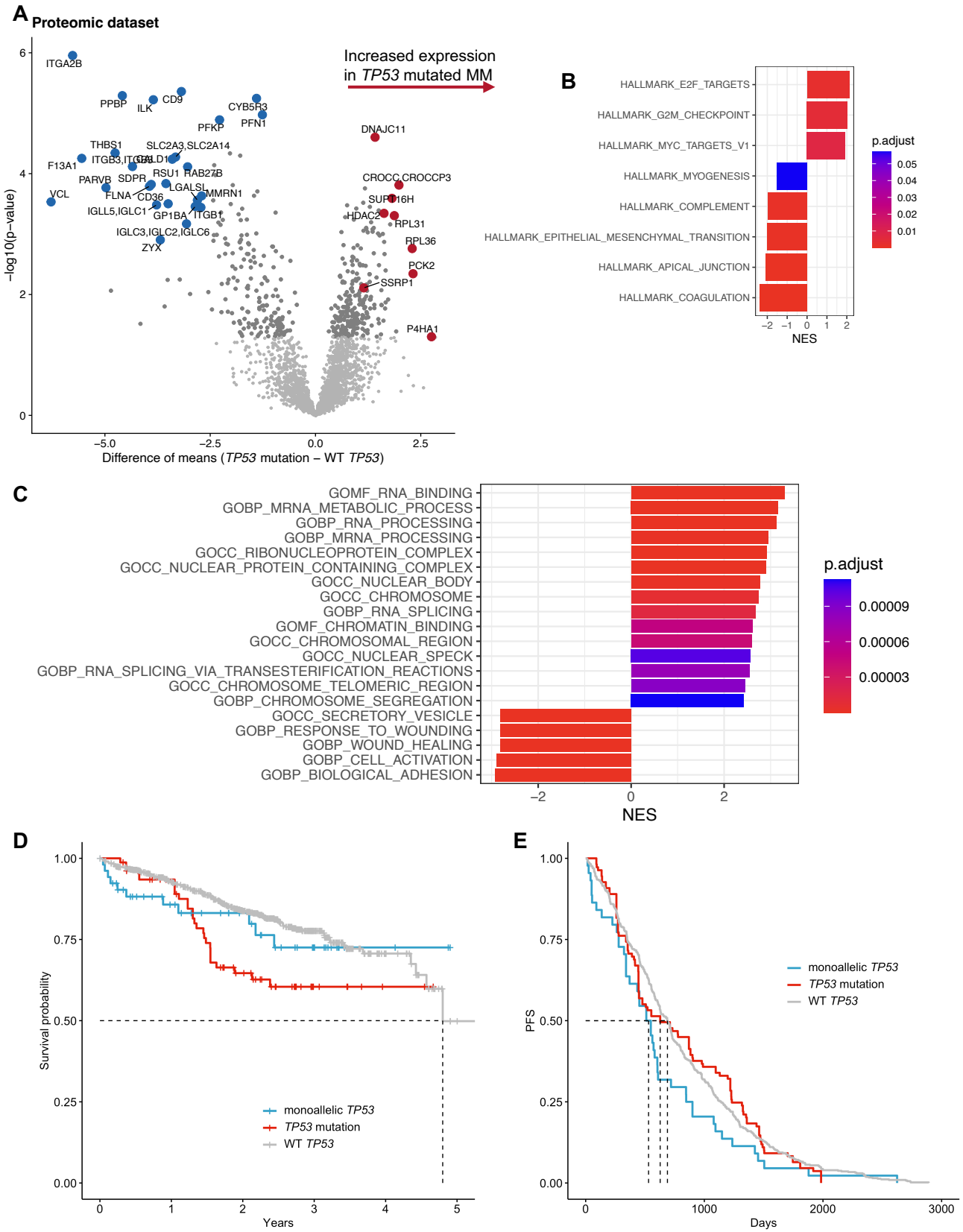
A
Proteomic dataset
Increased expression in TP53 mutated MM
ITGA2B
PPBP
ILK
CD9
CYB5R3
PFN1
PFKP
THBS1
SLC2A3,SLC2A14
F13A1
ITGB3,ITGA2B
ALD1
PARVB
SDPR
RSU1
RAB27B
VCL
FLNA
CD36
LGALSL
MMRN1
IGLL5,IGLC1
GP1BA
ITGB1
IGLC3,IGLC2,IGLC6
ZYX
DNAJC11
CROCC,CROCCP3
SUPT16H
HDAC2
RPL31
RPL36
PCK2
SSRP1
P4HA1
−log10(p−value)
Difference of means (TP53 mutation − WT TP53)
B
HALLMARK_E2F_TARGETS
HALLMARK_G2M_CHECKPOINT
HALLMARK_MYC_TARGETS_V1
HALLMARK_MYOGENESIS
HALLMARK_COMPLEMENT
HALLMARK_EPITHELIAL_MESENCHYMAL_TRANSITION
HALLMARK_APICAL_JUNCTION
HALLMARK_COAGULATION
NES
p.adjust
C
GOMF_RNA_BINDING
GOBP_MRNA_METABOLIC_PROCESS
GOBP_RNA_PROCESSING
GOBP_MRNA_PROCESSING
GOCC_RIBONUCLEOPROTEIN_COMPLEX
GOCC_NUCLEAR_PROTEIN_CONTAINING_COMPLEX
GOCC_NUCLEAR_BODY
GOCC_CHROMOSOME
GOBP_RNA_SPLICING
GOMF_CHROMATIN_BINDING
GOCC_CHROMOSOMAL_REGION
GOCC_NUCLEAR_SPECK
GOBP_RNA_SPLICING_VIA_TRANSESTERIFICATION_REACTIONS
GOCC_CHROMOSOME_TELOMERIC_REGION
GOBP_CHROMOSOME_SEGREGATION
GOCC_SECRETORY_VESICLE
GOBP_RESPONSE_TO_WOUNDING
GOBP_WOUND_HEALING
GOBP_CELL_ACTIVATION
GOBP_BIOLOGICAL_ADHESION
NES
p.adjust
D
Survival probability
Years
monoallelic TP53
TP53 mutation
WT TP53
E
PFS
Days
monoallelic TP53
TP53 mutation
WT TP53